

High productivity machining of holes in Inconel 718 with SiAlON tools

Aitor Arruti Agirreurreta^{1, a)}, Jose Angel Pelegay^{2, b)},
Pedro Jose Arrazola^{1, c)} and Klaus Bonde Ørskov^{2, d)}

¹ Faculty of Engineering, Mondragon University, Mondragon 20500, Spain
² Danish Advanced Research Centre, Sandagervej 10, 7400 Herning, Denmark

^{a)} epaitorr@gmail.com

^{b)} jap@damrc.com

^{c)} pjarrazola@mondragon.edu

^{d)} kbo@damrc.com

Abstract. Inconel 718 is often employed in aerospace engines and power generation turbines. Numerous researches have proven the enhanced productivity when turning with ceramic tools compared to carbide ones, however there is considerably less information with regard to milling. Moreover, no knowledge has been published about machining holes with this type of tools. Additional research on different machining techniques, like for instance circular ramping, is critical to expand the productivity improvements that ceramics can offer. In this a 3D model of the machining and a number of experiments with SiAlON round inserts have been carried out in order to evaluate the effect of the cutting speed and pitch on the tool wear and chip generation. The results of this analysis show that three different types of chips are generated and also that there are three potential wear zones. Top slice wear is identified as the most critical wear type followed by the notch wear as a secondary wear mechanism. Flank wear and adhesion are also found in most of the tests.

INTRODUCTION

Inconel 718 is a heat resistant alloy that exhibits an excellent mechanical strength and resistance to creep at high temperatures, good surface stability, and corrosion and oxidation resistance. One of the major drawbacks of this material is their low machinability. This is mainly due to their high ductility and work hardening, which means that the plastic deformations induced during the machining process generate a hardened and difficult to penetrate superficial layer. Moreover, as their mechanical properties are kept at high temperatures. Their low thermal conductivity make that temperature reached at the cutting edge is high. Besides, age hardening nickel alloys contain abrasive titanium and aluminium particles (1–3).

Although HSS have been used as tool materials, especially in interrupted cutting processes due to their high toughness, nowadays mainly carbides are employed (3,4). However, ceramic cutting tools are becoming more and more popular with the rise in demand for higher productivity, improvement in machine capabilities and growth in use of Heat Resistant Super Alloys (HRSA). The high hardness and abrasion resistance, ability to maintain hardness at high temperatures, chemical stability at high temperature and lower friction are the key of the success of ceramic tools with superalloys. These features enable the use of much higher cutting speeds than with carbides even in dry machining conditions, making possible to achieve higher material removal rates and a lower overall machining cost. Among the different types of ceramics, the most utilized ones to machine this type of materials are SiAlON and Al₂O₃+SiC whisker reinforced. There are some differences in their properties, like the higher hot-hardness and thermal shock resistance of SiAlONs, or the slightly higher fracture toughness of SiC_w ones. Even though, both have shown equal suitability for turning, while SiAlONs have the best performance in high-speed milling (5–7).

In general with ceramics tools, the adjustment of cutting parameters to each particular tool geometry must be done carefully, otherwise they are immediately destroyed due to their brittleness.

Many papers have analysed the behaviour of SiAlON tools when machining Inconel 718 superalloy. X. Tian et al. (8) studied the effects of cutting speed and up/down strategies when face milling. It was found that notch wear is the dominant failure mechanism at lower cutting speeds than 1400 m/min, while adhesion is the principal failure type at higher values than 1800 m/min. Flaking, abrasion and microcrack failures are also common. As a result, higher cutting speeds than 1000 m/min and up-milling are recommended to prolong tool life. L. Li et al (9) also utilized SiAlON ceramic inserts for carrying out turning tests in Inconel 718 and observed that at lower cutting speeds (120 m/min) they are prone to notch wear with minimum damage of the tool nose, while at 300 m/min notching is reduced and nose and flank wear increased. Zhao Jun et al. (10) studied failure mechanism of whisker-reinforced and SiAlON tools in turning nickel-base alloys, and concluded that the former have a higher nose and flank wear resistance due to their better chemical stability. It was also seen that, at higher cutting speed than 180 m/min, notch wear decreases considerably and catastrophic fracture of the edge due to plastic deformation may occur. G. Brandt et al. (11) also tested the turning of Inconel 718 with the previously mentioned two ceramic types, and found that the DOC notch wear resistance and the appearance of chipping along the edge line is equal for both. However, whisker-reinforced tools showed a better flank wear resistance due to their better chemical stability. M. Nablant et al. (12) studied different geometries when turning Inconel 718 with SiAlON ceramic tools, concluding that crater and flank wear are the dominant failures in square type inserts, while flank and notch wear are more common in round inserts.

Round inserts allow the possibility of applying different entering angles depending on the depth of cut, which enables a better control of the notch formation. Negative rake angles are usually utilized, due to the better force distribution and edge security that they offer. The edge preparation is also of special importance because a sharp edge can be easily cracked, and most of the ceramic tools are honed or chamfered. For general purpose turning, a T-land of 0.1 mm by 20° is commonly recommended by tool manufacturers, and for more demanding applications like milling, the latter can be combined with a honed edge, or the edge can be increased in the width and/or angle of the chamfer (7,13).

Most of the literature is focused in turning, while the high-speed milling with SiAlONs has rarely been analysed, been in most of the cases a face milling the studied case. Even though holes are traditionally machined by drilling, there are not commercially available ceramic drills. An alternative can be the use of circular ramping strategy, which consists in employing an indexable milling tool that follows a spiral tool path along the hole. This technique has not been tested with ceramic inserts in any paper and a further research in this area is necessary to extend the enhanced productivity of SiAlON ceramic tools to the machining of holes in Inconel 718.

EXPERIMENTAL PROCEDURES

Set up

Circular ramping milling operations were carried out in a Hermle C22U 5-axis CNC machining centre, whose maximum spindle speed was 18,000 rpm. The workpiece was clamped in a manual jaw chuck during all the tests. All the tests were carried in dry conditions but assisted with air flow. Thanks to this, the poor chip evacuation from the bottom of the hole (which caused the melting and catastrophic failure of the inserts in the first trials) was solved. The roughness was measured with a Marsurf PS1. Considering that the measured profile was periodic, it was based in the RS_m value to select the correct sampling length. The microscope to examine the chips and the tool wear was OITEZ brand's eScope DP-M07.

Experimental Plan

The machined holes were $D_m = 35\text{Ø}$ mm and 10 mm in length. The spiral movement was in counter clockwise direction combined with a clockwise rotation of the tool. The maximum chip thickness was kept constant at $h_{ex} = 0.05$ mm in all the experiments. Three different cutting speeds and pitch values of the spiral were used in the milling tests, 700, 1000 and 1414 m/min, and 0.8, 1.5 and 2 mm respectively. After defining the P and h_{ex} and making use of the Equation 1, the feed per tooth could be calculated, as well as the peripheral and tool center feed rates (Equation 2 and 3 respectively). The different combinations resulted in 9 tests and the cutting parameters of each one can be found in the Table 1. Each test was performed once and a completely new cutting edge was used in

each one to clearly distinguish the tool wear between them. Apart from the mentioned 9 tests, a final test of 50 mm in length was done at $V_c = 1414$ m/min and $P = 1.4$ mm to check the effect of machining longer holes. The chips were collected in every test.

$$f_z = \frac{D_m \cdot h_{ex} \cdot iC}{2D_{vf} \sqrt{a_p \cdot iC - a_p^2}} \quad (1)$$

$$V_{fm} = n \cdot f_z \cdot z_n \quad (2)$$

$$V_f = \frac{D_m - D_3}{D_m} \cdot V_{fm} \quad (3)$$

Workpiece Material and Employed Tool

For the milling tests, three workpieces of casted Inconel 718 were used. RPGN090300E-type SiAlON ceramic round inserts of $iC = 9.525$ mm size, made of CC6060 grade and manufactured by Sandvik Coromant were used in all the tests. The tool-holder was R300C-025A20-09M with an exterior diameter of $D_3 = 25$ mm, and the tests were carried out with the same number of inserts as it is capable of carrying, two.

Table 1. Testing parameters

Test N°	h_{ex} (mm)	P (mm)	f_z (mm/tooth)	V_c (m/min)	N (rpm)	V_{fm} (m/min)	V_f (m/min)	Data available
1	0.05	1.4	0.25	700	8913	4412	1260	Yes
2				1000	12732	6302	1801	Yes
3				1414	18000	8910	2546	No
4		0.9	0.31	1414	18000	10984	3138	No
5				700	8913	5439	1554	Yes
6				1000	12732	7769	2220	Yes
7		2.0	0.21	700	8913	3808	1088	Yes
8				1000	12732	5440	1554	Yes
9				1414	18000	7691	2197	Yes
10		1.4	0.25	1414	18000	8910	2546	No

RESULTS

3D Model

A 3D model was created to have a visual representation of the action of the tool in the circular ramping. This contributed to a better understanding of the results. As it is explained below, the tool rotates while follows a spiral oriented in the same longitudinal axis of the hole being machined. This movement results in the tool following a quite complex path. The 3D model was simplified performing a cut remaining the tool in the same position during one revolution. Then, this revolution cut was simulated every feed per tooth. The variations generated by different feed and pitch values were neglected, and it was supposed that the 3D model is similar in all the tests performed.

The shape of the chip is illustrated in the Figure 1.a. I was observed that the tool is constantly engaged with both the inner and outer part of the insert, making use of around 135° of the total cutting edge. That means that if a completely new cutting edge is required for each test, the insert can only be rotated once.

It was observed that h_{ex} is not constant during one full revolution of the tool. Cutting process (using the cutting parameters of the 10th test) was simulated every 10° of an insert round, and h_{ex} for each position are plotted in the Fig. 1.b. The blue line indicates that the h_{ex} in that position was located in the outer part of the insert, while the red one shows that it was in the inner part. The maximum chip thickness in a whole round was located at 75° in the outer part of the insert (Fig. 1.c) and there was a second maximum in the inner part at 260° .

An additional issue that was observed is that between 180° and 200° , as well as at 0° , the chip thickness fell to 0 mm. Although the values shown in the Fig. 1.a are specific for a particular combination of cutting parameters, the same tendency was repeated with any parameters for the actual D_3 and D_m .

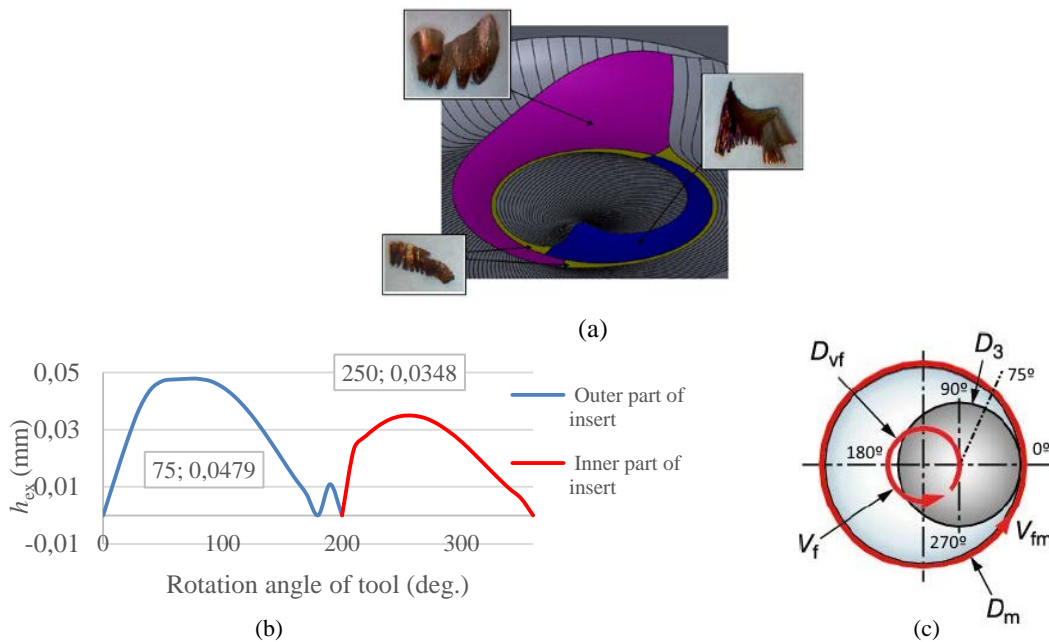


Figure 1. Three types of chips of a circular ramping (a), change of the h_{ex} in relation to the tool rotation (b) and visualization of the tool position when h_{ex} is maximum (c)

Chip Formation

Three different types were identified (Fig. 1). The first type of chips (pink) were generated when the insert was machining the periphery of the hole and this chip was the largest one in height due to the big engagement arc of the outer part of the insert. Although there was a difference in the concavity between the 3D drawing and the real chip, it could be due to the stresses generated by the high temperatures that make it bend. The second type (blue) was generated after the height of the chip had decreased and finished in the pike of the tip. In the end of this chip could be observed how the colour turns black due to the decreasing of the chip thickness as it gets closer to the tip. It was observed that the division between these two chips were very close to the angles at which the h_{ex} becomes 0 in Fig. 1.a. The third type of chips (yellow) were generated in the rest of the machined area and their height was almost constant. They were always burned, probably due to their small thickness.

Chip evacuation played an important role, and without any air supply, chips were melted and got stuck to the workpiece and the tool. Staying in cut showed the biggest effect, and there was a clear difference between the 9 tests (which lasted 7 - 12 s) and the 10th test (27 s). In the latter mentioned tests, the chips generated were less continuous, less smooth and less burnt with a matt grey colour in general.

Tool Wear

Three potential zones where the insert was worn out were found in the last test (Fig. 2), some of which matched with the rest of the tests. The first one was located in the exterior part of the tools. Despite the fact that flank wear was found in all the cutting edge, a concentrated flank wear was identified in that zone. Here, the effective diameter is the maximum, and therefore the cutting speed is maximum too. The higher cutting speed in the exterior part of the tool could lead to higher temperatures and therefore an accelerated abrasive wear mechanism (14). Moreover, one of the depth-of-cut lines (highest point of the pink chip) was next to that point and this still can generate stress concentrations, which end up in a notch wear as can be seen in the Fig. 3.a.

The second critic zone was only found in the last test, located in the bottom of the insert. The downward movement of the tool creates a compressive force in the flank face and the consequently increased friction could be the reason why a remarkable flank wear was also found in this area (Fig. 3.b). Moreover, unlike the rest of the cutting edge, this part of the insert was constantly engaged, which can also explain the extended flank wear.

The third zone was in contact with the tip generated in the centre, which was generated because the tool diameter was bigger than the radius of the hole. Therefore, the machining was also done with the inner part of the insert. Here the duration of the test also showed a strong effect. In the first 9 tests, flank wear and notching caused by the highest

point of the blue chip were found. However, in the test N° 10, a clear top slice wear was seen (Fig. 3.c), which matched exactly with the position of the tip (Fig. 2). The reason why the left insert from the Fig. 2 is rotated is to show how the flaking matches with this tip. The cutting speed in this zone was the lowest one compared with the rest of the cutting edge and this generated a lower temperature than in the rest of the cutting edge. Consequently, the workpiece material didn't soften enough and the cutting created higher pressure forces (15). The flaking off of small pieces around the top face of the cutting edge could also be caused by that pressure applied in an extended flank wear. A reason why no top slice was found in the short tests can be that the flank wear was not big enough to cause the top slice. Another cause can be that the notch wear was extended every time that the insert passed through the tip, so when the machining lasted longer, the notch wear was big enough to create a flaking in that area (4).

Apart from flank wear, some adhesion phenomena were also found all along the flank face, probably caused by the high temperatures that generated the tested high cutting speeds. Another reason could be that the cutting edge was not sharp enough because of the flank wear, and thus the metal was ploughed instead of cut (16).

The effect of different cutting parameters on tool wear was analysed as well. As refers to the cutting speed, although no major differences were found from 700 to 1000 m/min, the inserts used at 1414 m/min had considerably more adhered workpiece material (Fig. 4. a). Notch and flank wear were also higher, which can be explained with the previously mentioned "taking off" of the adhered material that removes material from the tool. The effect of the pitch was also analysed and no considerable changes in the wear were observed when $P = 0.8$ mm and 1.4 mm were used. However, a further increase of the pitch to 2 mm had a negative effect in the notch wear. Flank wear was also increased and the cutting edge was strongly fractured (Fig. 4. b). This pattern was repeated both at 700 and 1000 m/min, while pitch of 2 mm couldn't be checked at 1414 m/min due to the lack valid data.

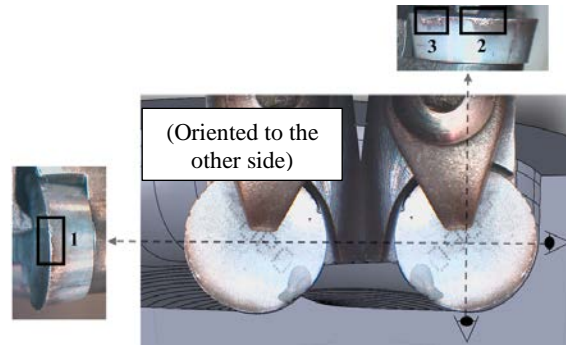


Figure 2. Identified three potential wear zones

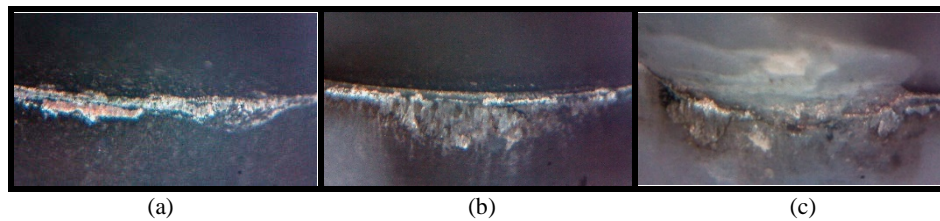


Figure 3. First (a), second (b) and third (c) potential wear zones

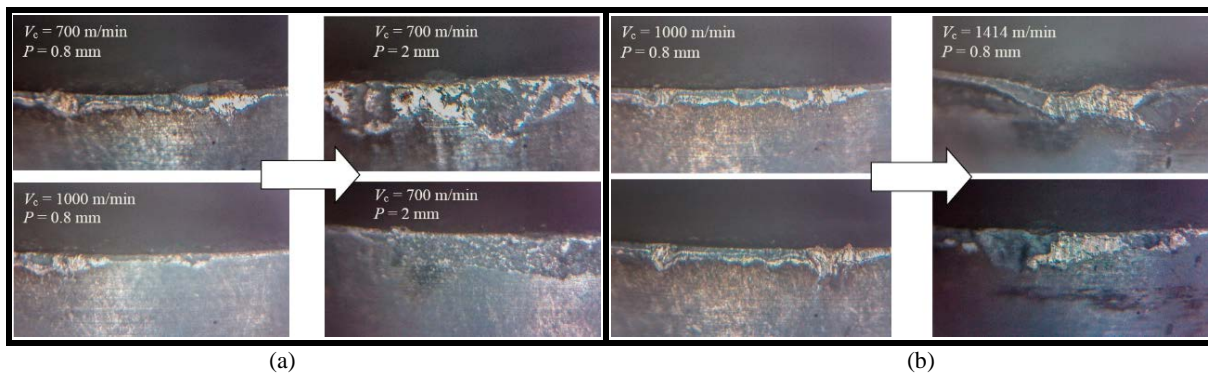


Figure 4. Effect of cutting speed (a) and pitch (b) in tool wear

CONCLUSIONS

- SiAlON 6060 Sandvik grade round inserts can be successfully used for machining holes in roughing with a circular ramping technique.
- Three different types of chips are generated due to the characteristic tool path of a circular ramping. Moreover, high cutting speeds and staying for a prolonged time in the cut has the strongest effect, generating a less burnt chip and a better chip breaking.
- Three potential wear zones have been identified with differences in wear patterns between them. The outer part of the insert was mainly affected by a notch wear, in the bottom part a remarkable flank wear has been observed, and in the inner part a top slice might be generated. Flank wear is found in all the cutting edge although it is not as much as in the bottom of the insert. Some adhered workpiece material was also found.
- At higher cutting speeds more adhesion phenomena has been found due to the increased temperatures in the cutting edge. However, the top slice is reduced if the cutting speed is increased due to the softening of the workpiece material and the resultant lower pressure forces in the cutting edge.
- Flank wear, notching and fracture of the cutting edge have a tendency to increase when pitch is increased from 1.4 mm to 2 mm. Therefore, a lower pitch than 1.4 is beneficial for the tool life in a circular ramping.

LITERATURE

1. Edward Trent, Paul Wright. Metal Cutting. Fourth edition. Butterworth Heinemann; 2000.
2. H. Z. Li, X. Q. Chen. 2. Tool Condition Monitoring in Machining Superalloys. In: Aerospace Materials Handbook. Taylor & Francis Group; 2013.
3. J. R. Davis. Machining of Nickel Alloys. In: Nickel, Cobalt, and Their Alloys. ASM International; 2000. p. 235–44.
4. E.O. Ezugwu, Z.M. Wang, A.R. Machado. Machinability of Nickel based super alloys: a review. In 1999.
5. Eckart Uhlmann. Cutting of Inconel and Nickel Base Materials. In: CIRP Encyclopedia of Production Engineering. Springer; 2014. p. 329–34.
6. E. Wiemann. Hochleistungsfräsen von superlegierungen [High-performance cutting of supra-alloys]. In Uhlmann E (ed) Berichte aus dem produktionstechnischen zentrum Berlin. Fraunhofer IRB Verlag, Germany; 2006.
7. Dev Banerjee, Raouf Ben Amor. Ceramic Cutting Tools. In: CIRP Encyclopedia of Production Engineering. Springer; 2014. p. 140–52.
8. X. Tian, J. Zhao, J. Zhao, Z. Gong, Y. Dong. Effect of cutting speed on cutting forces and wear in high-speed face milling of Inconel 718 with Sialon ceramic tools. In Springer; 2013.
9. L. Li, N. He, M. Wang, Z.G. Wang. High speed cutting of Inconel 718 with coated carbide and ceramic inserts. In 2002. p. 127–30.
10. Zhao Jun, Deng Jianxin, Zhang Jianhua, Ai Xing. Failure mechanisms of a whisker-reinforced ceramic tool when machining nickel-based alloys. In: 1997. Elsevier; p. 220–5.
11. G. Brandt, A. Gerendas, M. Mikus. Wear Mechanisms of Ceramic Cutting Tools When Machining Ferrous and Non-ferrous Alloys. In.
12. Muammer Nalbant, Abdullah Altin, Hasan Gökkaya. The effect of cutting speed and cutting tool geometry on machinability properties of nickel-base Inconel 718 super alloys. In Elsevier; 2007. p. 1334–8.
13. Choll K. Jun, Keith H. Smith. 6. Alumina-Silicon Carbide Whisker Composite Tools. In: Ceramic Cutting Tools: Materials, Development, and Performance. Noyes Publications; 1999. p. 86–111.
14. D. Dudzinski, A. Devillez, A. Moufki, D. Larrouquère, V. Zerrouki, J. Vigneau. A review of developments towards dry and high speed machining of Inconel 718 alloy. In 2004. p. 439–56.
15. I.A. Choudhury, M.A. El-Baradie. Machinability of nickel-base super alloys: a general review. In 1998. p. 278–84.
16. E.O Ezugwu, J. Bonney, Y. Yamane. An overview of the machinability of aeroengine alloys. In 2003. p. 233–53.